

Magnetic and Structural Study of $\text{Mn}_{1.15}\text{Fe}_{0.85}\text{P}_{1-x}\text{Ge}_x$ ($0.25 < x < 0.32$) Magnetocaloric Compounds Prepared by Arc Melting

L. HAWELEK^{a,*}, P. WŁODARCZYK^a, P. ZACKIEWICZ^a, M. POLAK^a, M. KAMINSKA^a,
R. PUŻNIAK^b, I. RADELYTSKYI^b AND A. KOLANO-BURIAN^a

^aInstitute of Non-Ferrous Metals, J. Sowińskiego 5, 44-100 Gliwice, Poland

^bInstitute of Physics, Polish Academy of Sciences, al. Lotników 32/46, 02-668 Warszawa, Poland

(Received May 13, 2015)

Recently, room temperature magnetocaloric materials increasingly attracted attention in the development of magnetic refrigerators. In this paper, an effect of P/Ge substitution on the magnetic phase transition in the series of $\text{Mn}_{1.15}\text{Fe}_{0.85}\text{P}_{1-x}\text{Ge}_x$ ($0.25 < x < 0.32$) magnetocaloric compounds prepared by the arc melting technique and subsequent homogenization process has been studied. Calorimetric and magnetization results show that the temperature of structural phase transition coincide with the Curie temperature and fall within the temperature range 270–355 K. The magnetic entropy change reaches the maximum value for the compound with $x = 0.28$ and equals to 32 J/(kg K) for the magnetic field change of 5 T. The adiabatic temperature change for the same sample, measured using magnetocalorimeter, is equal to 1.2 K for the magnetic field change of 1.7 T. It was found that the increase of Ge content in the sample causes weakening of first order magnetic transition, which is manifested by the lowering difference in transition temperature measured in two zero-field-cooling and field-cooled-cooling regimes.

DOI: [10.12693/APhysPolA.128.76](https://doi.org/10.12693/APhysPolA.128.76)

PACS: 75.30.Sg, 75.30.Kz, 61.05.C-, 61.66.Fn

1. Introduction

Magnetocaloric effect is defined as the effect of changing temperature of adiabatically isolated material under external magnetic field. Applying magnetic field to the material causes ordering of magnetic moments, which in consequence leads to the drop of magnetic entropy. Energy of the system is being conserved by the increase of temperature of material. Therefore, there are two quantities characterizing magnetocaloric effect (MCE) i.e. adiabatic temperature change (ΔT_{ad}) and magnetic entropy change (ΔS_{M}). The highest MCE can be achieved in the vicinity of magnetic transition temperature, especially near ferro- to paramagnetic transition. It is caused by the fact that magnetic entropy change given by the equation: $\Delta S = \int_{B_i}^{B_f} \left(\frac{\partial M}{\partial T} \right)_B dB$ depends on the derivative of magnetization with respect to temperature. In other words, abrupt change of magnetization causes increase of magnetic entropy change. Adiabatic temperature change of material depends on the magnetic entropy change, but also on its heat capacity (in magnetic field) and transition temperature. It is given by the relation [1]:

$$\Delta T_{\text{ad}} = - \int_{B_i}^{B_f} \frac{T}{C_B} \left(\frac{\partial M}{\partial T} \right)_B dB,$$

where T denotes Curie point, C_B is a heat capacity in the vicinity of magnetic transition in the magnetic field with an induction B . As the ΔT_{ad} depends on ΔS , T and C_B , it is more appropriate to compare ΔT_{ad} between different materials instead of comparing ΔS .

At present, there are several interesting groups of magnetocaloric materials, which are good candidates for active regenerator material used in room temperature cooling devices. The first group of materials are hydrogenated as well as cobalt doped lanthanum based $\text{La}(\text{Fe},\text{Si})_{13}$ intermetallic compounds. The second one is related to the manganese-based compounds, mainly Fe_2P type compounds such as $(\text{Mn},\text{Fe})_2(\text{P},\text{X})$ [$\text{X} = \text{Ge}, \text{Si}, \text{As}$] [2–5], but also manganites [6, 7]. In Ref. [8] one can find comparison of three types of materials i.e. pure gadolinium (Gd), $\text{La}(\text{Fe},\text{Si},\text{Co})_{13}$ and manganite with composition $\text{Pr}_{0.65}\text{Sr}_{0.35}\text{MnO}_3$. Performance of these materials was tested in prototype in different operating conditions. It turned out that every tested material has its own advantages and there is no simple answer which material is better. However it is known the fact that the minimal requirement for a material for use in magnetic refrigerator is the value of adiabatic temperature change equal to 1 K under magnetic field $B = 1$ T [9].

The magnetocaloric features of $\text{MnFe}(\text{P}_{1-x}\text{Y}_x)$ compounds were for the first time reported by Tegus et al. in the $\text{MnFeP}_{0.45}\text{As}_{0.55}$ [2]. In further studies, the same authors have shown impact of changing P/As ratio on the Curie temperature and magnetic entropy change [5]. Arsenic was also substituted for germanium, which caused drop in the MCE and increase of T_c [3]. In the latest results presented for the Fe_2P

*corresponding author; e-mail:
lukasz.hawelek@imm.gliwice.pl

family of compounds, adiabatic temperature change was measured directly by Yibole et al. [10]. It was found that the adiabatic temperature change drops in the series $MnFe(P,As) > MnFe(P,Si) > MnFe(P,Ge)$. It is striking that the magnetic entropy change drops in the reversed order than the ΔT_{ad} (highest ΔS_M values were reported for $MnFe(P,Ge)$), which indicates strong influence of latent heat on magnetocaloric effect. In all the studied $MnFe(P,Ge)$ compounds first order magnetoelastic transition (FOMT) has been reported. Until now, there are many papers published that introduce magnetocaloric effect in the $MnFe(P,Ge)$ series with respect to the composition changes [11–15].

The aim of this study was to show new method of preparation $MnFePGe$ compounds (arc melting) and to investigate an effect of composition of $MnFe(P,Ge)$ on the crystal structure, the phase transition temperature, adiabatic temperature change ΔT_{ad} , magnetic entropy change ΔS and phase transition hysteresis.

2. Experimental details

Approximately 3 g samples were prepared by arc melting technique (Edmund Buhler MAM-1, Germany) from pure elements and compounds (Mn 3N pieces, Fe 3N wire, Mn_3P_2 3N pieces, Fe_2P 3N and Ge 5N). Buttons were remelted six times under the protective gas and then homogenized for the next 50 h at 923 K under the vacuum 5×10^{-5} mbar (wire vacuum furnace, Czylok, Poland). Thereafter, samples were slowly cooled down by furnace to the room temperature. The phase purity and the crystal structures were determined by powder X-ray diffraction (XRD) using $Ag K_\alpha$ radiation (D/MAX RAPID II-R Rigaku Denki Co. Ltd., Japan). The microstructures were observed by energy dispersive spectroscopy (EDS) and wavelength dispersive spectroscopy (WDS) (JCSA 733, JEOL, Japan). Magnetic measurements were performed using a Superconducting Quantum Interference Device (SQUID) magnetometer. The magnetic entropy changes $\Delta S_M(T,B)$ were calculated from isothermal magnetization curves ($M-B$ curves) in the vicinity of the Curie temperature using the thermodynamic Maxwell relation using so called “loop process” [16]. The isothermal magnetization curves were measured in a temperature range of 230–350 K under magnetic fields of 0–5 T. The adiabatic temperature changes $\Delta T_{ad}(T,B)$ were obtained with an adiabatic magnetocalorimeter (AMT&C Group, Russia) in a temperature range of 170–350 K under magnetic field 1.7 T. The external magnetic field was changed in a cycle 0–1.7 T–0 with a rate of 1 T/s during ΔT_{ad} measurements. Adiabatic isolation during ΔT_{ad} measurements was ensured by vacuum equal to 2×10^{-2} mbar. Structural phase transition hysteresis was obtained by means of calorimetric methods. Thermal analysis was performed with use of Netzsch Pegasus 404c equipped with silver furnace and liquid nitrogen cooling system. Heating and cooling runs were conducted with the 10 K/min rates under helium atmosphere (gas flow equal to 50 mL/min).

3. Results and discussion

In present work, five different samples with different amount of germanium were studied:

- 1 — $Mn_{1.15}Fe_{0.85}P_{0.76}Ge_{0.25}$,
- 2 — $Mn_{1.15}Fe_{0.85}P_{0.74}Ge_{0.26}$,
- 3 — $Mn_{1.15}Fe_{0.85}P_{0.72}Ge_{0.28}$,
- 4 — $Mn_{1.15}Fe_{0.85}P_{0.70}Ge_{0.30}$,
- 5 — $Mn_{1.15}Fe_{0.85}P_{0.68}Ge_{0.32}$.

At the beginning, EDS was employed in order to check the structure of obtained samples. This method is known to be effective in showing the presence of micro-segregations. The EDS maps for all the samples (Fig. 1, for selected sample) have given us the phase composition in the microscale and the elemental analysis for each phase. For all the samples Fe_2P -type (> 85%) phase was dominating one, while two other minor phases i.e. $FeMnGe$ and MnO were also confirmed.

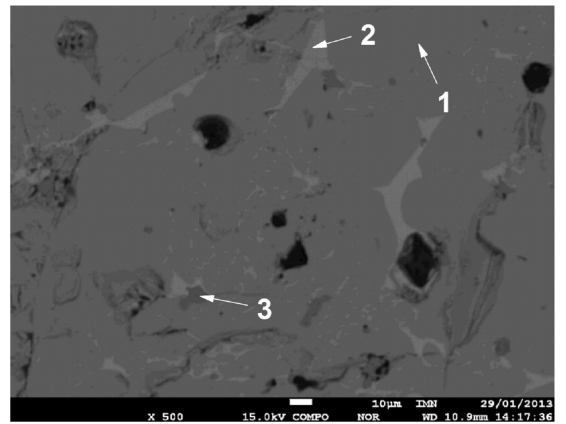


Fig. 1. Microstructure of sample 1. Fe_2P -type phase (1) dominates in the microstructure, but two additional phases as impurities are clearly shown (2 — $Fe_3Mn_4Ge_6$, 3 — MnO).

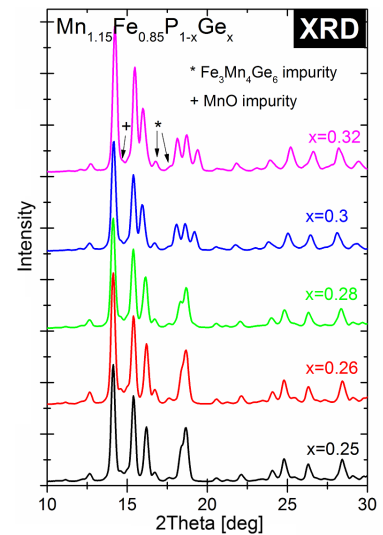


Fig. 2. Room temperature X-ray diffraction patterns. The main peaks that originate from impurities are marked on the patterns.

TABLE I

Phases weight fractions, room temperature lattice parameters, c/a ratio and unit-cell volume V for Fe_2P -type phase obtained via Rietveld refinement. The sample with the highest V value is marked in bold.

Sam-ple	Fe_2P -type [%]	MnO [%]	$\text{Fe}_3\text{Mn}_4\text{Ge}_6$ [%]	$a = b$ [Å]	c [Å]	c/a ratio	V [Å ³]
1	91.55 ± 1.09	4.52 ± 0.66	3.93 ± 0.46	6.0690 ± 0.0006	3.4492 ± 0.0005	0.5683	110.027 ± 0.017
2	85.82 ± 0.79	7.00 ± 0.51	7.17 ± 0.51	6.0659 ± 0.0005	3.4501 ± 0.0004	0.5687	109.941 ± 0.019
3	93.12 ± 1.40	4.30 ± 0.81	2.59 ± 0.58	6.0916 ± 0.0006	3.4372 ± 0.0005	0.5643	110.461 ± 0.027
4	89.26 ± 1.24	6.27 ± 0.72	4.47 ± 0.50	6.1666 ± 0.0005	3.3585 ± 0.0004	0.5446	110.608 ± 0.026
5	89.80 ± 1.71	1.35 ± 0.33	8.84 ± 0.60	6.1463 ± 0.0006	3.3266 ± 0.0005	0.5412	108.837 ± 0.022

The room temperature powder X-ray diffraction patterns for all the studied compounds have been shown in Fig. 2. They can be indexed mainly in the hexagonal Fe_2P -type structure with the $P62m$ space group. In this structure, the Mn atoms occupy the $3g$ sites, the Fe atoms occupy the $3f$ sites, and the P and Ge atoms occupy randomly the $1b$ and $2c$ sites. There are also indications of two impurity phases $\text{Fe}_3\text{Mn}_4\text{Ge}_6$ (the $P6/mmm$ space group) and MnO (the $Fm-3m$ space group), which were also confirmed by EDS analysis. MnO impurity probably originates from the oxidation of Mn during the preparation process. The phases weight fraction, room temperature lattice parameters, unit-cell volume V and c/a ratio were then calculated using the Rietveld refining method [17] as implemented in the FullProf program [18] and presented in Table I. Three compositions 1, 2, 3 are paramagnetic at room temperature, whereas samples 3 and 4 are ferromagnetic at room temperature. This is indicated by the differences on diffraction patterns (Fig. 2) in the range of $17.5\text{--}20^\circ$. The smaller c/a ratio for the samples 4 and 5 results from the magnetostriction effect occurring at the Curie temperature, which is in agreement with the previous results [19, 20].

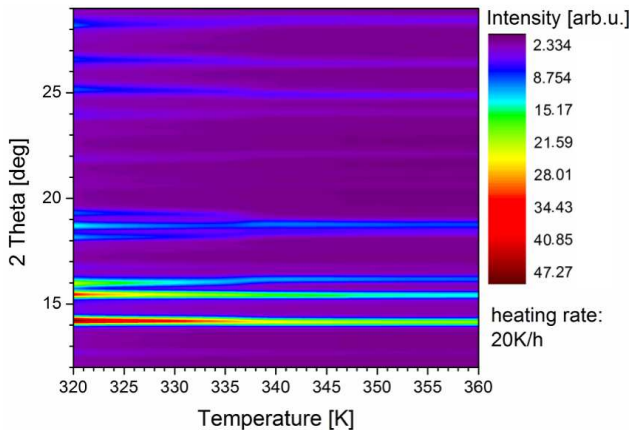


Fig. 3. Temperature dependent X-ray diffraction two-dimensional pattern measured for sample 4.

The temperature dependent powder X-ray diffraction pattern in 2θ range from 5 to 35° of the sample 4 is shown in Fig. 3. It is clearly seen that peaks positions are changing continuously during the heating, which indicates that the phase transition is of magnetoelastic type, without any symmetry change. The structural phase transition occurs in the temperature range of 10 K from 330 to 340 K under the heating rate 20 K/h.

Magnetic measurements in the magnetic field up to 5 T were performed on three of the five studied samples 1, 4 and 5 differing by the germanium content. For all the samples the temperatures of magnetic phase transitions were estimated from magnetization measurements, which were conducted by use of two different regimes i.e. ZFC (zero-field-cooling) and FCC (field-cooled-cooling). In Table II transition temperatures obtained from ZFC (corresponds to Curie temperature) and FCC measurements were presented. It is commonly accepted that if the sample can be undercooled in magnetic field below its Curie point, the magnetic transition is of the first order type (FOMT). In such situation difference between ZFC and FCC transition temperatures will be observed. Moreover, the higher the ZFC–FCC hysteresis, the stronger is the first order character of transition. As one can see, the ZFC–FCC hysteresis is correlated with the Ge/P ratio. Changing germanium amount from $x = 0.25$ to $x = 0.32$ causes lowering ZFC–FCC hysteresis from 13 to 4 K, thus increased concentration of germanium is related to weakening first order transition. By performing calorimetric measurements, structural transition temperatures were obtained. In Table II, onset temperatures of transitions, which are independent on heating/cooling rates, obtained in both cooling and heating regimes have been shown. As one can notice, temperatures of structural transitions are lower than the Curie temperatures obtained from magnetization measurements. The difference in temperatures does not exceed 10 K. For all measured samples, hysteresis between onset temperatures of structural transitions measured in cooling and heating modes has been reported. The hysteresis depends on Ge/P ratio and is higher in samples with lower amount of germanium (3.4 K for $x = 0.25$).

TABLE II

Onset temperatures and temperature hysteresis ΔT_{DSC} estimated from calorimetric measurements compared with the temperature hysteresis ΔT_{M} calculated from ZFC and FCC measurements.

Sam-ple	Onset T — cooling [K]	Onset T — heating [K]	ΔT_{DSC} [K]	T_{ZFC} [K]	T_{FCC} [K]	ΔT_{M} [K]
1	266.7	270.1	3.4	276	263	13
2	273.1	275.8	2.7	284	272	12
3	316.2	318.2	2.0	322	314	8
4	328.7	330.5	1.8	336	330	6
5	341.8	343.1	1.3	346	342	4

In Fig. 4 the Arrott and magnetic entropy change plots for all three samples are gathered. The Arrott diagrams

were prepared with the use of critical exponents adapted from the mean field theory i.e. $\beta = 0.5$ and $\gamma = 1$. In all three cases curves on the plots have negative slope, therefore according to the Banerjee criterion [21] all these magnetic phase transitions can be classified as a first order type (FOMT). From the inspection of the Arrott plots it can be seen that the negative slope is changing with the Ge/P ratio. Hence the first order character of magnetic transition is diminished while Ge/P ratio is increasing which is also in agreement with the decreasing value of the ZFC–FCC hysteresis. Magnetic entropy change calculated from the magnetization curves at low magnetic fields (up to 1 T) increases with the amount of germanium. The increase of germanium from 0.25 to 0.30 in the composition is related to the increase of magnetic entropy change from 4 to 7 J/(kg K). At higher magnetic fields samples numbered as 4 and 5 ($x_{Ge} = 0.30$ and $x_{Ge} = 0.32$) have equal values of magnetic entropy change $|\Delta S_M| = 13$ J/(kg K). Therefore, suppression of first order transition character is correlated with the increase of magnetic entropy change at low magnetic fields. One can also observe that the dependence of magnetic entropy change on the magnetic field is closer to linear for samples with higher amount of germanium.

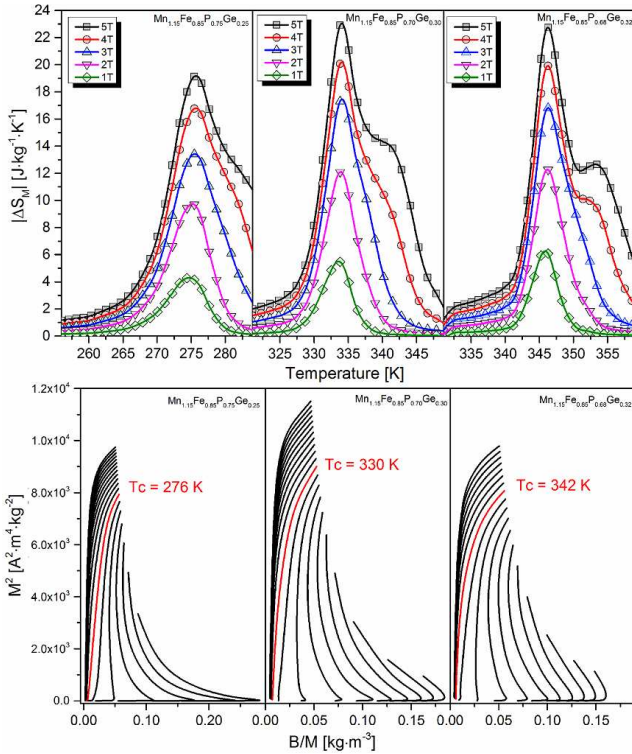


Fig. 4. Arrott plots (bottom) and magnetic entropy changes (top) for samples 1, 4 and 5.

To further evaluate the performance in terms of refrigeration efficiency, we have computed the refrigerant capacity (RC). The RC parameter reflects the amount of heat energy that can be transferred from the cold to

the hot end of a refrigerator in one thermodynamic cycle, and it is defined as integral [1]:

$$RC = \int_{T_1}^{T_2} \Delta S(T) dT,$$

where T_1 and T_2 indicate the half width span of the curve. From the practical point of view, the RC parameter is as important as the maximum of ΔT_{ad} .

TABLE III

RC values calculated for samples 1, 4 and 5.

Sample	RC [J/kg]		
	$B = 1$ T	$B = 2$ T	$B = 3$ T
1	24.3	57.0	99.3
4	22.3	55.7	97.3
5	22.6	53.8	91.7

In Table III calculated values of RC in the function of B for sample 1, 4 and 5 are compared. From the practical point of view, it is very beneficial to obtain large magnetic entropy changes and high RC for low magnetic fields (0.5–2 T) as such fields can be realized by using NdFeB permanent magnets in prototyped room temperature magnetic refrigerators. In present work, RC parameter has been calculated for magnetic fields with induction $B = 1, 2,$ and 3 T i.e. up to field that can be treated as permanent magnet limit. Note that the RC values are almost not sensitive to Ge/P ratio and are equal to about 55 J/kg in 2 T. For higher field (3 T) calculated value for sample 1 and 4 is slightly higher than for sample 5 and reaches 99,97 and 92 J/kg for samples 1, 4, and 5, respectively. The origin of such difference in RC value comes from the various asymmetric broadening of the entropy change maxima calculated from isothermal magnetic measurements, which can be caused by the samples heterogeneities.

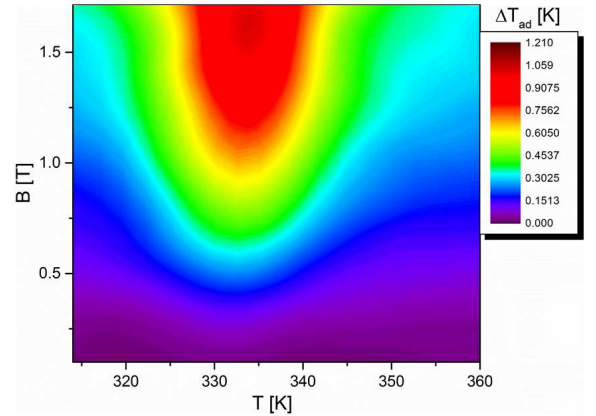


Fig. 5. Map of the adiabatic temperature change for sample 4 in heating regime.

In Fig. 5, the adiabatic temperature change was visualized via the thermal map. The isothermal measurements were performed in the heating regime for sample 4

($x_{\text{Ge}} = 0.30$). As one can see, adiabatic temperature change equal to 1.2 K at magnetic field change $B = 1.7$ T was reported. It can be easily noticed that the area on the map of high values of adiabatic temperature change is quite small. The half width of the two-dimensional curve plotted for magnetic field $B = 1.7$ T is quite narrow (about 10 K).

4. Conclusions

Impact of the Ge/P ratio in the series of $\text{Mn}_{1.15}\text{Fe}_{0.85}\text{P}_{1-x}\text{Ge}_x$ intermetallic compounds, obtained via arc melting technique and subsequent homogenization, on the crystal structure, phase transition and magnetocaloric effect has been studied. The increase of the Ge/P ratio causes diminishing of the first order phase transition character and decrease of the phase transition hysteresis. Compounds with higher amount of germanium have not only higher magnetocaloric effect in the field up to 5 T but also much higher Curie point. However, from the application point of view the refrigerant capacity value up to 3 T is only slightly sensitive on Ge/P value. Additionally, for the magnetic refrigeration technology the adiabatic temperature change for the sample with the highest unit cell volume and composition $\text{MnFeP}_{0.7}\text{Ge}_{0.3}$ has been directly measured under the magnetic field 1.7 T and reached 1.2 K at 334 K.

Acknowledgments

Lukasz Hawelek acknowledges for a grant from the National Science Center, Poland (2011/01/D/ST5/07816).

References

- [1] K.A. Gschneidner Jr., V.K. Pecharsky, A.O. Tsokol, *Rep. Prog. Phys.* **68**, 1479 (2005).
- [2] O. Tegus, E. Bruck, K.H.J. Buschow, F.R. de Boer, *Nature* **415**, 150 (2002).
- [3] W.X. Li, O. Tegus, L. Zhang, W. Dagula, E. Bruck, K.H.J. Buschow, F.R. de Boer, *IEEE Trans. Magn.* **39**, 3148 (2003).
- [4] O. Tegus, E. Bruck, W.X. Li, L. Zhang, W. Dagula, F.R. de Boer, K.H.J. Buschow, *J. Magn. Magn. Mater.* **272–276**, 2389 (2004).
- [5] O. Tegus, E. Bruck, L. Zhang, W. Dagula, K.H.J. Buschow, F.R. de Boer, *Physica B* **319**, 174 (2002).
- [6] V. Dyakonov, A. Slawska-Waniewska, J. Kazmierczak, K. Piotrowski, O. Iesenchuk, H. Szymczak, E. Zubov, S. Myronova, V. Pashchenko, A. Pashchenko, A. Shemjakov, V. Varyukhin, S. Prilipko, V. Mikhaylov, Z. Kravchenko, A. Szytula, W. Bazela, *Low Temp. Phys.* **35**, 568 (2009).
- [7] A. Szewczyk, H. Szymczak, A. Wisniewski, K. Piotrowski, R. Kartaszynski, B. Dabrowski, S. Kolesnik, Z. Bukowski, *Appl. Phys. Lett.* **77**, 1026 (2000).
- [8] U. Legait, F. Guilou, A. Kedous-Lebouc, V. Hardy, M. Almanza, *Int. J. Refrig.* **37**, 147 (2014).
- [9] K.G. Sandeman, *Scr. Mater.* **67**, 566 (2012).
- [10] H. Yibole, F. Guillou, L. Zhang, N.H. van Dijk, E. Bruck, *J. Phys. D Appl. Phys.* **47**, 075002 (2014).
- [11] W. Dagula, O. Tegus, B. Fuquan, L. Zhang, P.Z. Si, M. Zhang, W.S. Zhang, E. Bruck, F.R. de Boer, K.H.J. Buschow, *IEEE Trans. Magn.* **41**, 2778 (2005).
- [12] A. Yan, K.H. Muller, L. Schultz, O. Gutfleisch, *J. Appl. Phys.* **99**, 08K903 (2006).
- [13] D. Liu, M. Yue, J. Zhang, T.M. McQueen, J.W. Lynn, X. Wang, Y. Chen, J. Li, R.J. Cava, X. Liu, Z. Altounian, Q. Huang, *Phys. Rev. B* **79**, 014435 (2009).
- [14] M. Yue, Z.Q. Li, X.B. Liu, H. Xu, D.M. Liu, J.X. Zhang, *J. Alloys Compd.* **493**, 22 (2010).
- [15] E. Bruck, O. Tegus, L. Zhang, X.W. Li, F.R. de Boer, K.H.J. Buschow, *J. Alloys Compd.* **383**, 32 (2004).
- [16] L. Caron, Z.Q. Ou, T.T. Nguyen, D.T. Cam Thanh, O. Tegus, E. Brück, *J. Magn. Magn. Mater.* **321**, 3559 (2009).
- [17] H. Rietveld, *Acta Crystallogr.* **22**, 151 (1967).
- [18] J. Rodriguez-Carvajal, *Physica B* **192**, 55 (1993).
- [19] H. Yabuta, K. Umeo, T. Takabatake, K. Koyama, K. Watanabe, *J. Phys. Soc. Japan* **75**, 113707 (2006).
- [20] M.T. Sougrati, R.P. Hermann, F. Grandjean, G.J. Long, E. Brück, O. Tegus, N.T. Trung, K.H.J. Buschow, *J. Phys. Condens. Matter* **20**, 475206 (2008).
- [21] S.K. Banerjee, *Phys. Lett.* **12**, 16 (1964).